INTERACTION OF CRATER EJECTA WITH ATMOSPHERE. N. A. Artemieva[1] and J. V. Morgan[2], [1]Planetary Science Institute, Tucson USA, artemeva@psi.edu; [2]Imperial College, London UK, j.v.morgan@imperial.ac.uk.

Introduction: A standard scenario for the emplacement of the K-Pg boundary ejecta layer assumes a combination of two mechanisms: 1) ballistic emplacement of mainly molten target material that travels within an ejecta curtain up to a distance of ~4000 km; 2) precipitation of projectile/target condensates from a global (much larger than the Earth's radius) vapor plume. It appears, however, that this scenario is inconsistent with observational data, for example the presence of shocked quartz in the K-Pg layer which would be annealed within the plume, as well as advanced numerical simulations which show that there is not enough high-velocity ejecta to form the global layer. An alternative hypothesis of more global ejecta being emplaced from an ejecta curtain is also inconsistent with observational data since: 1) ballistic ejecta thin with distance from the crater and the global layer has a roughly constant thickness; 2) if the impact were oblique the ejecta would be thicker downrange and the ejecta has a fairly symmetrical distribution; 3) material in an ejecta curtain is compressed to a range of shock pressures, while the global layer is principally formed from impact spherules. Ambient global winds were considered as a possible mechanism for ejecta emplacement in pioneering studies of the K-Pg layer [1-3]. We have previously suggested that ejecta are re-distributed through a powerful interaction with the atmosphere [4]; a mechanism that was originally proposed to explain rings in Jupiters's atmosphere caused by the collision with Shoemaker-Levy 9 fragments [5].

In this paper we model ejecta/atmosphere interaction for craters with transient cavity diameters from 1 to 90 km and compare the results with terrestrial records (Ries and Chicxulub craters in particular). Our preliminary results show that the atmosphere is able "to accelerate" ejecta from large craters and re-distributes them to much larger distances. The ultimate goal of the study is to apply similar methods to craters on other planets, where a dense atmosphere (Venus) or volatile-rich target (Mars) results in unusual crater forms.

Methods: We use the multi-phase hydrocode SOVA [6], which is a 2D/3D Eulerian code that models multidimensional, multi-material, large deformation, strong shock wave physics, coupled with the ANEOS equation of state. The code has the capability to model dusty flows – the interaction of solid or molten particles with gas. In this method, each fragment is characterized by its individual parameters (mass, density, position, and velocity) and is subjected to gravity and drag. Additionally, the particles exchange heat with the atmosphere via convection and conduction. Size-frequency distribution (SFD) of particles is described by a power law $N_{>m}=Cm^{-b}$ with the exponent b=0.8 (large fragments prevail, LF) or 1.1 (small fragments prevail, SF). Minimum fragment size is 10 µm whereas maximum fragment size is defined by maximum shock compression: if shock compression is <60 GPa (solid ejecta) it could as large as tens of m; particles subjected to shock pressures 60-150 GPa are treated as "melt" with maximum size of 1 cm; particles compressed above 150 GPa represent a vapor-melt mixture and has a narrow SFD with the largest particle size of 200 µm.

Ballistic versus non-ballistic deposition. We start with a simplified approach by neglecting crater formation process, using scaling laws [7] for the initial mass-velocity distribution of ejecta, and by assigning the same size of 100 µm to all ejected particles (which is incorrect for low-velocity ejecta but is appropriate for high-velocity molten and partially vaporized ejecta).

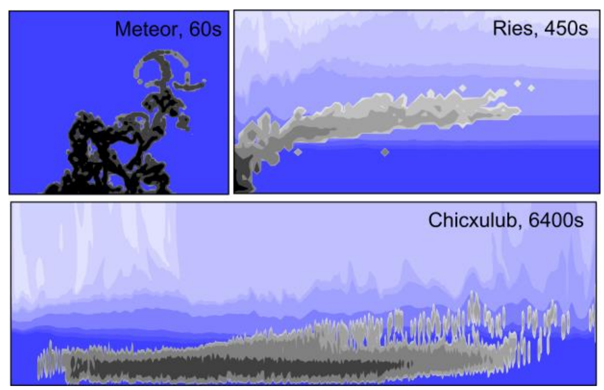

Fig. 1. Ejecta cloud for craters with different D_{tc}. Shading of gray shows dust density; shading of blue – density of the atmosphere. The Meteor frame is 6×5 km; Ries frame is 800×80 km; Chicxulub frame - 4000×80 km. Crater center is at the bottom left corner of each frame. The Chicxulub cloud is still in motion.

We find, as expected, that ejecta from the smallest crater (D_{tc}=1km) are restricted to 8 crater diameters: two minutes after impact remnants of the ejecta curtain are transformed into a highly turbulent cloud which slowly settles to the ground (its input into already deposited ejecta is minimal). In contrast, within the first hour after the largest impact (D_{tc} = 90 km), ballistic ejecta are already deposited) residual particles form a thick (tens of km) cloud which moves outward horizontally with a velocity of 10-100 m/s (the cloud is likely to be turbulent on the sub-cell scale, but is not resolvable in our simulations). To some extent this cloud is similar to pyroclastic density currents in volcanology, and the atmosphere is dense enough to provide "volatiles" that drive the flow, but span huge distances. Ejecta from an intermediate in size crater (D_{tc} = 8 km) combine characteristics of both cases: on the one hand, a highly turbulent cloud exists in the crater vicinity; on the other hand, a sub-horizontal layer of particles moves slowly outward. The ejecta thickness for all three cases is shown in Fig. 2.

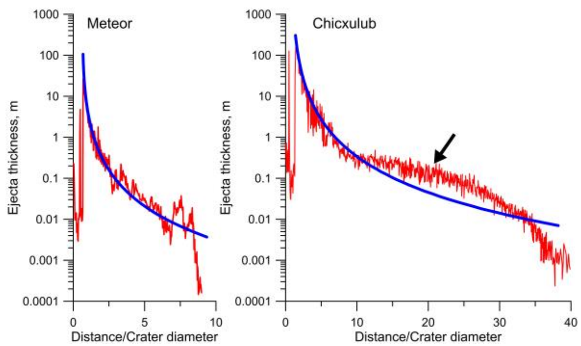

Fig. 2. Ejecta blanket thickness for a small crater (left) and a large crater (right). Red lines show calculated values (particles in the cloud have been extrapolated to the surface); blue lines show the case for ejecta deposited ballistically (i.e. with no atmosphere).

Comparison with observations. A quickly expanded debris clouds in atmosphere have been observed during the Shoemaker-Levy 9 collision with Jupiter [8]. A similar mechanism has been modelled for the Tunguska event to predict dispersion of the projectile material and formation of noctilucent clouds [9]. Although initial conditions are different (an airburst versus a cratering event), terrestrial atmosphere is dense enough to modify a small fraction of the finest crater ejecta.

Ries crater. In our calculations a small non-ballistic ejecta component exists, but it is too thin to generate the suevitic breccia layer that is observed outside and inside Ries crater [10]. At least part of the distal cloud could form moldavite deposits.

Double K-Pg layer in North America, global ejecta, and Chicxulub suevite. The ejecta thickness at distances > 1000 km (Fig. 2) is affected by the atmosphere: the decrease in thickness with distance (red curve) is slower than for ballistic ejecta (blue curve). Vaporization of re-entering ejecta [11] as well as local winds could further homogenize the cloud during its slow descend to the ground. The modelled thickness of the fall-back ejecta does not exceed 10 m, and is much thinner than observed [12]. Similar to the Ries case, another mechanism is required to produce the suevitic layer, for example by MFCI.

Chicxulub ejecta in 3D. We model a hypothetical 60° Chicxulub-like impact [13] and at an altitude of 40 km replace tracers by representative particles with prescribed SFDs. Unavoidably, the 3D simulations are performed at a lower resolution than the 2D ones, and are only run for ~15 minutes after the impact. Nonetheless, we see the same tendency as in 2D simulations: thick near-crater (distance to deposition of 500-1000 km) ejecta move outward (and uprange) from the crater to be deposited at larger distances . At the end of LF simulations (b=0.8) 60% of ejecta are deposited, 38% are in the still moving cloud, and 2% are still in space (above 200 km altitude). In SF simulations (b=1.1) we see an opposite proportion: 57% are still in the cloud and 41% - on the ground. In both cases the cloud consists mainly from sediments (90%); the projectile and basement materials represent only 10% and have the mass ratio of ~2:1.

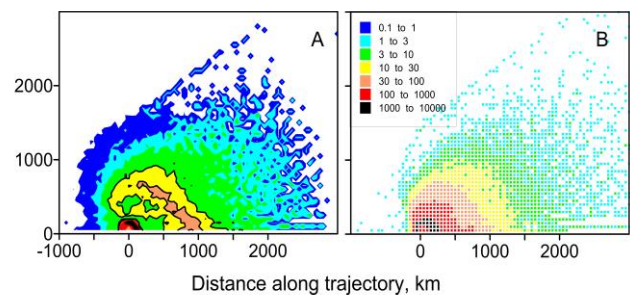

Fig. 4. Ejecta thickness in cm after a 60° impact (from left to right) producing a 90-km diameter transient cavity. A: 3D calculations with b=0.8. B: ballistic continuation. Only one half of the ejecta blanket is shown.

Acknowledgements. This study is supported by Exobiology NASA grant NNX16AI30G

References: [1] Alvarez L. W. et al. (1980) *Science*, *208*, 1095-1108. [2] Bohor B. F. et al. (1987) *Science*, *236*, 705-709. [3] Pope K. O. (2002). *Geology*, *30*, 99-102. [4] Artemieva N. A. and Morgan J. V. (2009). *Icarus, 201*, 768-780. [5] Colgate and Petschek (1985). [6] Shuvalov V. V. (1999*) Shock waves*, *9*, 381-390. [7] Housen K. R. and Holsapple K.A. (2011) *Icarus*, *211*, 856-875. [8] Hammel H. B. et al. (1995) *Science*, *267*, 1288-1296. [9] Artemieva N. and Shuvalov V. (2016) *AREPS*, *44*, 37-56. [10] Stöffler D. et al. (2013) *M&PS*, *48*, 515-589. [11] Artemieva N. and Morgan J. (2018) *LPSC-49*, Abstr. #2221. [12] Morgan J.V. et al. (2016) *Science*, *354*, 878-882 [13] Artemieva N. and Morgan J. (2017) *GRL*, *44*, 10,180-10,188.